Chen *et al. Geoscience Letters* (2022) 9:21
https://doi.org/10.1186/s40562-022-00227-w

Geoscience Letters

RESEARCH LETTER

Open Access

Feasibility study on artificial preparation of structured loess

Huie Chen[1], Hui Li[1], Yaling Jiang[2], Qingbo Yu[1*], Meng Yao[1] and Wenchong Shan[1]

Abstract

Structure collapse and subsidence are non-negligible geotechnical problems in loess areas. Within this framework, homogeneous and undisturbed samples are critical for effective research on loess structure. Hence, a novel method for preparing artificial structured loess (ASL) was proposed. The calcium oxide (CaO) was added to air-dried natural loess (NL) to form calcium carbonate ($CaCO_3$) cementation and the ASL samples with various densities were successfully prepared. Further, the microstructure test, shear test, and collapsibility test were conducted on the NL and ASL samples for feasibility analysis. Results show that compared with the NL, enough $CaCO_3$ could also be generated in the ASL samples with effective cementation among loess particles; the ASL presented similar compositional and structural characteristics and higher shear strength. The collapsibility of ASL was affected by its density: collapse would not occur when the density exceeded a certain threshold.

Keywords: Microstructure, $CaCO_3$ cementation, Collapsibility, Shear strength

Introduction

For clayey soils, the structure considered as the combination and particle arrangement (Mitchell 1976), could raise the strength and stiffness of soil and allow the natural soil to exist at a higher volumetric state than the reconstituted soil. As a typically structured soil, loess is characterized as loose, open-structured and collapsible (Li et al. 2020). Accordingly, collapsibility is a large concern in foundation design that deals with loess-like subsoil, as differential collapse deformations in loess could cause cracks in upper structures (Li et al. 2016). However, during sample collection, the structure of natural soil is likely to be damaged by sampling disturbance. Moreover, impurities such as gravel and plant roots render natural structured soils inhomogeneous and affect the study of soil structural behaviour. Against this backdrop, scholars have explored the feasibility and effectiveness of preparing artificial soils. The research shows that the artificial structured soil has more homogenous structure and higher strength, which is more suitable for the study of soil structure (Consoli et al. 2020; Konstantinou et al. 2021; Wang et al. 2020; Jiang et al. 2012).

Maccarini (University of London, UK) first prepared artificial sands using combustion method. Thereafter, various kinds of structured soils were prepared by adding different additives to the raw soil material to form cementation connection. The additives include cement (Yao et al. 2018; Consoli et al. 2020), mixture of cement and ice particles (Jiang et al. 2017), copper slag (Bharati and Chew 2016), gypsum (Wang et al. 2020), industrial salt (Liu et al. 2017), fly ash (Singhi et al. 2016), kaolin (Liu et al. 2017), and other materials (Konstantinou et al. 2021). Some researchers mixed CaO with original soil, compacted the mixture in layers to make samples, vacuum saturated the samples and then injected CO_2 or wrapped the samples with enough drikold to form $CaCO_3$ cementation between particles (Jiang et al. 2012; Yu and Liu 2020).

As $CaCO_3$ is the main cementation material in NL, the addition of cement and other materials may change the composition of the prepared soil and cause certain

*Correspondence: yuqb@jlu.edu.cn

[1] College of Construction Engineering, Jilin University, Changchun 130026, China
Full list of author information is available at the end of the article

property differences. During the sample preparation process of using CaO, the saturated sample needs to be air-dried to the designed moisture content, causing shrinkage of the sample; additionally, sublimation of drikold will cause a certain frost heave of the sample. Therefore, it is of significance to conduct further research on the preparation of ASL to ensure that the prepared samples have similar compositions and structural features to NL.

Given the paucity of existing research, a novel method for preparing ASL was proposed: mixed loess materials (air-dried NL mixed with CaO and water) were placed in a humid environment containing a high concentration of CO_2 to generate $CaCO_3$ cementation between loess particles. Meanwhile, the differences in engineering properties between ASL and NL were explored through microstructure test, shear test, and collapsibility test. Finally, the effectiveness of the proposed method of ASL was verified.

Materials and methods

Sample preparation

The raw material of ASL samples was NL blocks collected from Dongjiahe Town, Tongchuan City, Shaanxi Province, China (Fig. 1). The content of $CaCO_3$ planned to be generated in ASL is 16.7%. Since the natural density of Chinese loess is between 1.35 and 1.70 g/cm^3, three groups of samples (labelled as ASL1, ASL2, and ASL3) with different densities were prepared to verify the wide applicability of this method. Twelve samples were prepared for each group, including two for water content test, two for $CaCO_3$ content test, two for microstructure test, four for shear test, and two for collapsibility test. The main physicochemical properties of the samples are summarized in Table 1. Replicates were tested for each sample with the parallel error < 0.5% and the mean value was taken as the final result. Overall, the measured $CaCO_3$ content is closed to the target value (16.7%) though the heterogeneity of loess could slightly reduce the effective $CaCO_3$ content (Table 1).

Figure 2 shows the process of sample preparation. In the beginning, the NL blocks were crushed with a wooden hammer and air-dried. Particles larger than

Table 1 Physicochemical parameters of the samples

Property	NL	ASL1	ASL2	ASL3	Method
Water content (%)	16.7	16.7	16.7	16.7	ASTM D2216
Density (g/cm^3)	1.49	1.35	1.49	1.70	ASTM D7263
$CaCO_3$ content (%)	16.7	32.6	32.5	32.7	ASTM D4373
The newly generated $CaCO_3$ content (%)	0	15.9	15.8	16	ASTM D4373

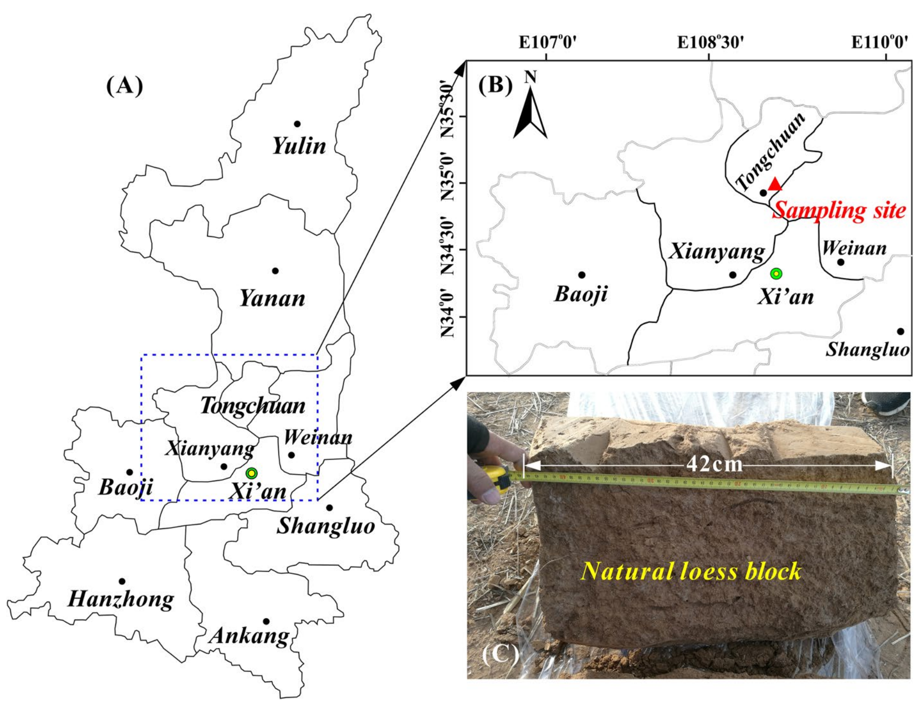

Fig. 1 Details of the sampling site. **A**, **B** Geographical location of the sampling area; **C** natural loess block

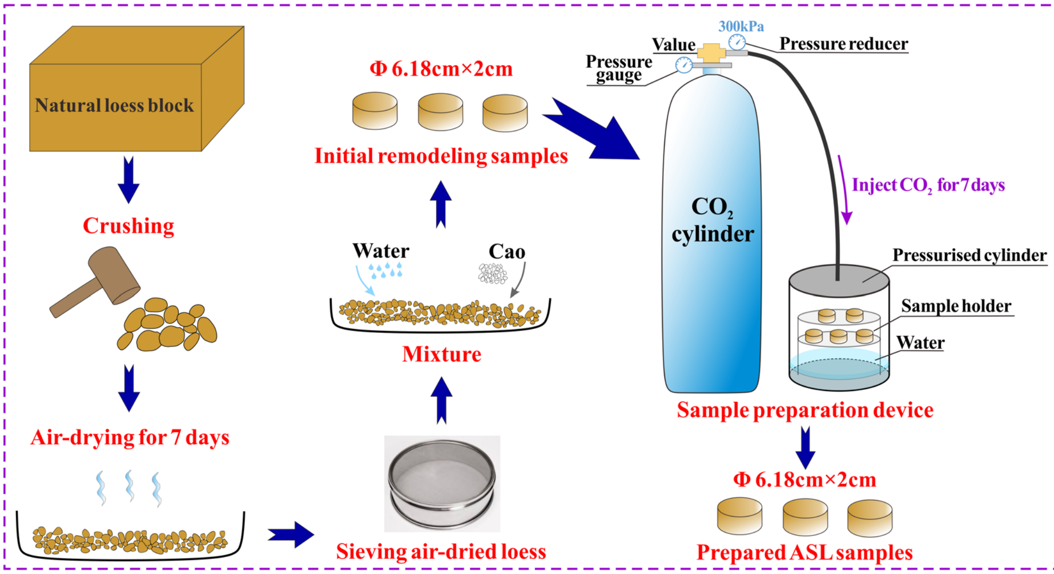

Fig. 2 The preparation process of ASL samples

0.5 mm in diameter were removed by sieving. Then, CaO and water were added to the air-dried loess to obtain a mixture. The required mass of air-dried loess (m_d), CaO (m_c), and water (m_w) were calculated as follows:

$$m_d = (1 + 0.01\omega_d)(1 - 0.01n)\frac{m}{1 + 0.01\omega}, \quad (1)$$

$$m_c = 0.56 \cdot 0.01n \cdot \frac{m}{1 + 0.01\omega}, \quad (2)$$

$$m_w = m - \frac{0.01w * m}{1 + 0.01\omega} + m_{w\mathrm{CaO}}, \quad (3)$$

where m is the mass (g) of mixed loess material, ω is the target water content (16.7%), w_d (%) is the water content of air-dried loess, n is the $CaCO_3$ content planned to be generated in ASL (16.7%), 0.56 is the factor used to convert $CaCO_3$ to the equivalent chemical relative atomic mass of CaO, and $m_{w\mathrm{CaO}}$ is the mass (g) of water consumed by the reaction between CaO and water. The mixture was pressed into the cutting rings by static pressure to prepare initial remodelling samples. The samples were placed in a pressurized cylinder with a certain amount of water at the bottom to create a humid environment. Then sealed the pressurized cylinder and inject CO_2 for 7 days according to the trial test, during which a pressure reducer was used to control the pressure at 300 kPa to maintain the concentration of CO_2. Accordingly, CaO was gradually consumed to generate $CaCO_3$ (Eqs. 4, 5):

$$\mathrm{CaO + H_2O \rightarrow Ca(OH)_2} \quad (4)$$

$$\mathrm{Ca(OH)_2 + CO_2 \rightarrow CaCO_3 + H_2O} \quad (5)$$

Testing methods

Microstructure tests, including scanning electron microscopy (SEM) and energy dispersive spectroscopy (EDS), were conducted on a Phenom ProX desktop scanning electron microscope. The samples were treated by the vacuum freeze-drying method to eliminate the influence of moisture on the microstructure observation (Delage and Pellerin 1984). To clarify the macroscopic strength characteristics of the samples, the shear tests were carried out using a ZJ strain-controlled direct shear apparatus produced by Nanjing Ningxi Soil Instrument Co. Ltd. The shear strength indices of samples were obtained by linear fitting (ASTM 2006). The collapsibility of samples was tested by the double line method on a GDG-4S consolidation apparatus produced by Nanjing Soil Instrument Factory. The collapse potential (I_c) was calculated as follows (ASTM D5333, 2006):

$$I_c = \frac{h_1 - h_2}{h_o} \times 100\%, \quad (6)$$

where h_1 and h_2 are the stabilized heights of a sample at in situ and saturated states under a vertical pressure, respectively; h_o is the initial height of a sample.

Results and discussion

EDS and SEM analysis

EDS analysis

Point analysis and map analysis (analytical EDS methods) were applied to the samples. From Fig. 3A, the rod calcite in the NL sample was distributed around the contacts between particles and induced a certain cementing effect. Since the NL has undergone exposure over a long-term geological history, there were many fine particles covered the calcite's surface, so there were certain amounts of silicon, iron, and aluminium in these calcite agglomerations. The $CaCO_3$ agglomerations in the ASL samples were well crystallized due to the better preparation environment and were mainly cubic, fusiform, or film-like. These $CaCO_3$ crystals bound loess particles together to generate a certain cementing effect.

Figure 3B shows the distribution of $CaCO_3$ in the ASL samples. In the samples, oxygen can be found in various minerals, calcium may exist in unreacted CaO or $Ca(OH)_2$, and carbon may exist in $CaCO_3$ or $MgCO_3$. Therefore, the distribution of $CaCO_3$ was determined by combining the distributions of carbon and calcium. The amount of cubic $CaCO_3$ was small, and there were no large-scale crystals in the samples. Fusiform $CaCO_3$ often coexisted with film-like $CaCO_3$ covering its surface and they were widely distributed throughout the samples. In addition, film-like $CaCO_3$ were wrapped on the surface of particles, cementing the fine clays on the skeleton units, or wrapping multiple particles together to form agglomerates. The newly generated $CaCO_3$ played a key role in the cementation between loess particles.

Microstructure characteristics

Figure 4 shows the microstructure characteristics of the samples at 800 and 2000 magnification. Both the NL sample and ASL samples presented skeletal structures (dominated by silts). Accordingly, the macropores (marked in red) could be well observed. From Fig. 4A, there were many clay–silt aggregates (marked in blue) around the macropores. However, due to lack of or weak cementation, the bonds between aggregates are easily destroyed under external load, resulting in larger deformation. As shown in Fig. 4B, the newly generated $CaCO_3$ were mainly distributed in the contact area between the particles to form cementations (marked in green). This indicates that the proposed method for preparing ASL can form effective $CaCO_3$ cementation between loess particles. In addition, due to the removal of impurities such as roots and stones, the structure of ASL is more homogeneous than that of NL. The ASL had similar compositional and structural features to NL.

Shear behaviour

Figure 5A shows the fitting curves of shear strength of NL and ASL samples. As presented in Fig. 5A, the shear strength of ASL samples with different densities was much higher than that of the NL sample. Moreover, the difference in the shear strength between ASL and NL samples rises with the increase of pressure. From Table 2, the cohesion (c) and internal friction angle (ϕ) of the ASL samples with different densities were also higher than the NL sample. $CaCO_3$ cementations can form a more effective and stable structure than matrix suction and soluble salt, which plays an important role in loess strength and deformation (Wei et al. 2020; Jiang et al. 2014). Through

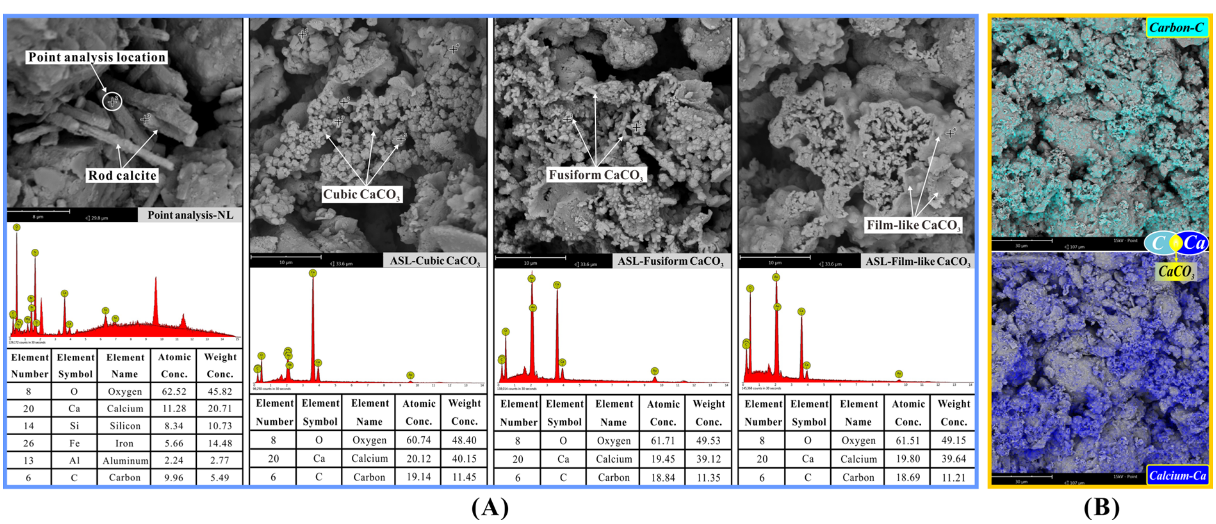

Fig. 3 EDS results of samples **A** $CaCO_3$ crystal form and **B** EDS map analysis-based typical carbon–calcium distribution of ASL sample

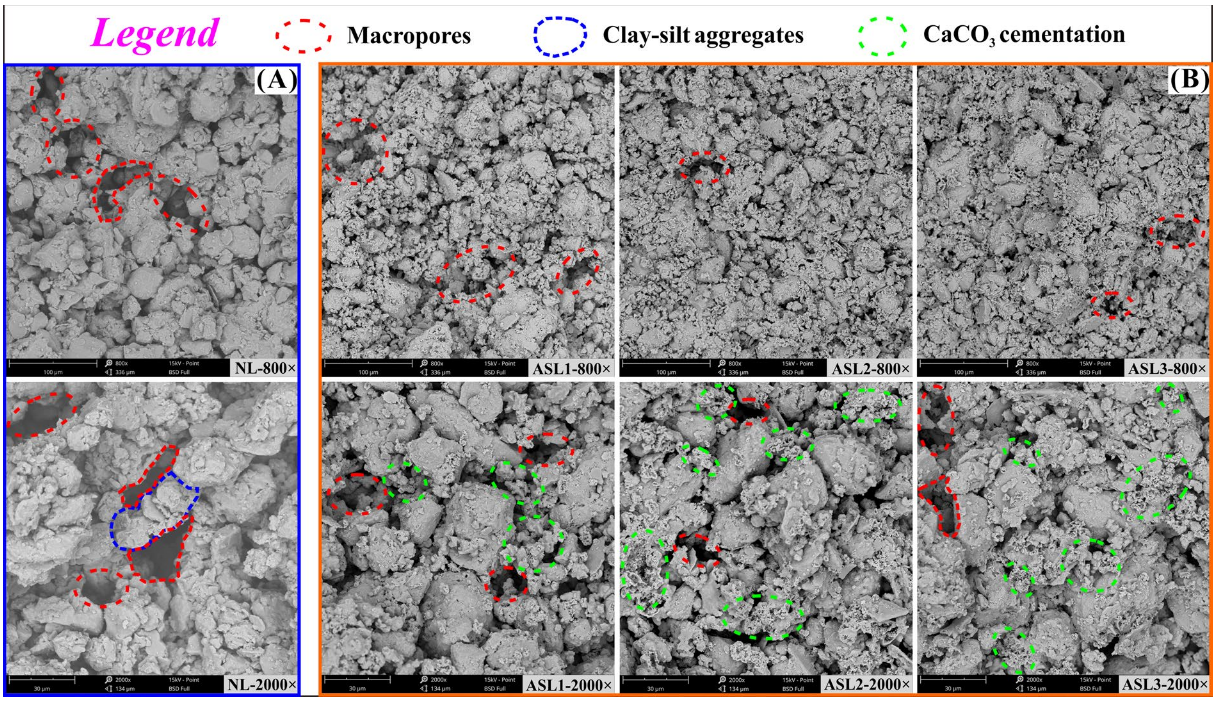

Fig. 4 Representative SEM images of the **A** NL and **B** ASL samples

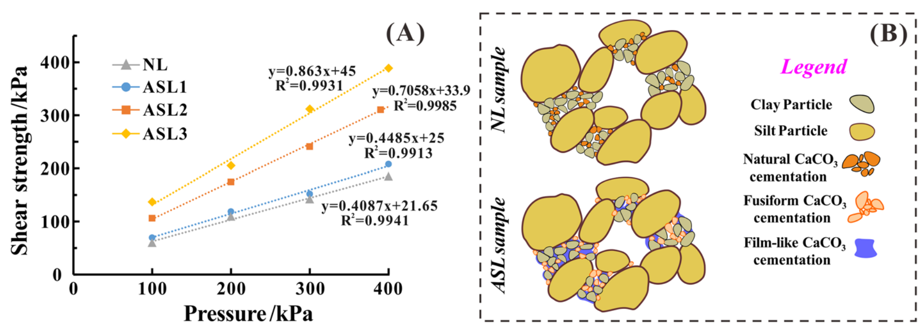

Fig. 5 **A** Fitted shear strength; **B** micro-schematic diagram of the NL and ASL samples

Table 2 Shear strength indices of the samples

Shear strength index	NL	ASL1	ASL2	ASL3
c/kPa	21.7	25.0	33.9	45.0
φ/°	22.2	24.2	35.2	40.8

the analysis of the microstructure of NL and ASL samples, it can be seen that there were many $CaCO_3$ crystals in ASL, which adhered to the loess particles and increased their surface roughness. Moreover, the formation of agglomerates, the fine clay particles cemented to skeletal particles by film-like $CaCO_3$, led to increased bond strength and particle surface roughness (Fig. 5B). Therefore, the shear strength and shear strength indices of ASL and NL samples follow the aforementioned rules.

Collapsibility characteristics

Figure 6 shows the variation of collapse potential of each sample with pressure. The collapse index (I_e) is the collapse potential at an applied vertical stress of 200 kPa, and the degree of sample collapse was classified according to their collapse index (ASTM 2006), as shown in Table 3. The occurrence of collapse settlement in loess requires two conditions to be satisfied simultaneously:

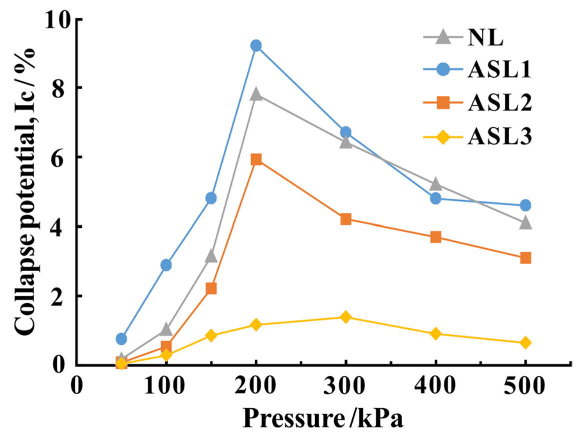

Fig. 6 Variation of the collapse potential with pressure

Table 3 Collapsibility test results of the samples

Property	NL	ASL1	ASL2	ASL3
I_e/%	7.8	9.2	5.9	1.2
Degree of sample collapse	Moderately severe	Moderately severe	Moderate	Slight

connection characteristics that were weakened in water and sufficient space for collapse. The looser the sample, the larger the collapsibility deformation, so the collapsibility of ASL1 was greatest. Since ASL exhibited a higher degree of crystallization of $CaCO_3$ compared with NL, its cementation effect was stronger. Moreover, film-like $CaCO_3$ wrapped fusiform $CaCO_3$ and other grains, and the $CaCO_3$ had strong water resistance, which reduced the water sensitivity of the samples. The combined action made the ASL2 and ASL3 samples have smaller collapse indexes and collapse degrees.

Conclusions

In this work, a novel method for preparing ASL samples was proposed. The following conclusions can be drawn:

1) The ASL samples presented similar compositional and structural features to the NL sample. The newly generated $CaCO_3$, concentrated at contact points among loess particles, were widely distributed in the ASL samples, resulting in more effective cementation. Both ASL and NL samples had skeletal structures with macropores, but the structure of ASL was more homogenous.
2) Since the fusiform and film-like $CaCO_3$ in ASL improved the connection between particles and surface roughness of the particles, the shear strength and shear strength indices of ASL exceeded that of NL. The collapsibility of ASL was related to its density, and its collapse degree was more severe when the density was low. Moreover, grains were wrapped by film-like $CaCO_3$, which reduced the water sensitivity of the sample. This made the collapse index of ASL smaller than that of NL with the same density.

To sum up, the ASL prepared by the proposed method had the same characteristics as NL without changing its composition and the ASL was suitable for the study of soil structure. The successful preparation of ASL facilitates a better understanding of the geotechnical and geophysical properties for the structured loess, providing a scientific basis for the treatment of loess foundation and the prevention of geological disasters.

Acknowledgements

The authors are grateful for the financial support of the study presented in this paper from the National Natural Science Foundation of China (Grant No. 41472242). The authors would also like to thank the reviewers and the associate editor for their valuable comments, which have improved the quality of this paper.

Author contributions

HEC analysed data and revised manuscript; HL contributed to analysis and manuscript preparation; YLJ initiated the idea of this study; QBY revised manuscript. Other authors helped analyse data. All authors read and approved the final manuscript.

Funding

The work was supported by the National Natural Science Foundation of China (No. 41472242).

Availability of data and materials

Not applicable.

Declarations

Competing interests

The authors declare that they have no competing interests.

Author details

[1]College of Construction Engineering, Jilin University, Changchun 130026, China. [2]Jilin Jianzhu University, Changchun 130026, China.

Received: 11 September 2021 Accepted: 10 April 2022
Published online: 17 May 2022

References

ASTM (2006) Annual book of ASTM standards. ASTM International, West Conshohocken

Bharati SK, Chew SH (2016) Geotechnical behavior of recycled copper slag-cement-treated singapore marine clay. Geotech Geol Eng 34:835–845. https://doi.org/10.1007/s10706-016-0008-8

Consoli NC, Da Silva A, Barcelos AM, Festugato L, Favretto F (2020) Porosity/cement index controlling flexural tensile strength of artificially cemented soils in Brazil. Geotech Geol Eng 38:713–722. https://doi.org/10.1007/s10706-019-01059-w

Delage P, Pellerin FM (1984) Influence de la lyophilisation sur la structure d'une argile sensible du Quebec. Clay Min 19:151–160. https://doi.org/10.1180/claymin.1984.019.2.03

Jiang MJ, Hu HJ, Liu F (2012) Summary of collapsible behaviour of artificially structured loess in oedometer and triaxial wetting tests. Can Geotech J 49:1147–1157. https://doi.org/10.1139/t2012-075
Jiang MJ, Zhang FG, Hu HJ, Cui YJ, Peng JB (2014) Structural characterization of natural loess and remolded loess under triaxial tests. Eng Geol 181:249–260. https://doi.org/10.1016/j.enggeo.2014.07.021
Jiang MJ, Li T, Cui YJ, Zhu HH (2017) Mechanical behavior of artificially cemented clay with open structure: cell and physical model analyses. Eng Geol 221:133–142. https://doi.org/10.1016/j.enggeo.2017.03.002
Konstantinou C, Biscontin G, Jiang NJ, Soga K (2021) Application of microbially induced carbonate precipitation to form bio-cemented artificial sandstone. J Rock Mech Geotech Eng 13:579–592. https://doi.org/10.1016/j.jrmge.2021.01.010
Li P, Vanapalli S, Li TL (2016) Review of collapse triggering mechanism of collapsible soils due to wetting. J Rock Mech Geotech Eng 8:256–274. https://doi.org/10.1016/j.jrmge.2015.12.002
Li YR, Shi WH, Aydin A, Beroya-Eitner MA, Gao GH (2020) Loess genesis and worldwide distribution. Earth-Sci Rev 201:102947. https://doi.org/10.1016/j.earscirev.2019.102947
Liu BS, Zhang YJ, Wang X, Liang QG, Li S (2017) Research on the collapsibility influencing factors and micro-mechanism of artificial loess. Chin J Undergr Space Eng 1313(02):330–336
Mitchell JK (1976) Fundamentals of soil behavior. Soil Sci Soc Am J 40:827–866. https://doi.org/10.2136/sssaj1976.03615995004000040003x
Singhi B, Laskar AI, Ahmed MA (2016) Investigation on soil-geopolymer with slag, fly ash and their blending. Arab J Sci Eng 41:393–400. https://doi.org/10.1007/s13369-015-1677-y
Wang WY, Wei DH, Gan YX (2020) An experimental investigation on cemented sand particles using different loading paths: failure modes and fabric quantifications. Constr Build Mater 258:119487. https://doi.org/10.1016/j.conbuildmat.2020.119487
Wei YN, Fan W, Yu B, Deng LS, Wei TT (2020) Characterization and evolution of three-dimensional microstructure of Malan loess. CATENA 192:104585. https://doi.org/10.1016/j.catena.2020.104585
Yao K, Xiao HW, Chen DH, Liu Y (2018) A Direct assessment for the stiffness development of artificially cemented clay. Géotechnique 69:1–23. https://doi.org/10.1680/jgeot.18.t.010
Yu HJ, Liu EI (2020) Cyclic properties of artificially cemented gravel-silty clay mixed soils. Exp Tech 44:573–589. https://doi.org/10.1007/s40799-020-00376-7

Publisher's Note